Available online at www.sciencedirect.com
SCIENCE DIRECT®
Vision Research 46 (2006) 932–939
Vision Research
www.elsevier.com/locate/visres

Resolution for spatial segregation and spatial localization by motion signals

David Burr [a,b,*], Suzanne McKee [c], Concetta M. Morrone [d]

[a] *Dipartimento di Psicologia, Università di Firenze, Via S. Nicolò 89, Italy*
[b] *Istituto di Neuroscienze del CNR, Via Moruzzi 1, Pisa 56100, Italy*
[c] *The Smith-Kettlewell Eye Research Institute, 2318 Fillmore Street, San Francisco, CA 94115, USA*
[d] *Facoltà di Psicologia, Università Vita-Salute San Raffaele, Via Olgettina 58, Milano 20132, Italy*

Received 20 July 2005; received in revised form 20 September 2005

Abstract

We investigated two types of spatial resolution for perceiving motion-defined contours: grating acuity, the capacity to discriminate alternating stripes of opposed motion from transparent bi-directional motion; and alignment acuity, the capacity to localize the position of motion-defined edges with respect to stationary markers. For both tasks the stimuli were random noise patterns, low-pass filtered in the spatial dimension parallel to the motion. Both grating and alignment resolution varied systematically with spatial frequency cutoff and speed. Best performance for grating resolution was about 10 c/deg (for unfiltered patterns moving at 1–4 deg/s), corresponding to a stripe resolution of about 3′. Grating resolution corresponds well to estimates of smallest receptive field size of motion units under these conditions, suggesting that opposing signals from units with small receptive fields (probably located in V1) are contrasted efficiently to define edges. Alignment resolution was about 2′ at best, under similar conditions. Whereas alignment judgment based on luminance-defined edges is typically 3–10 times better than resolution, alignment based on motion-defined edges is only 1.1–1.5 times better, suggesting motion contours are less effectively encoded than luminance contours.

Keywords: Vision; Motion contours; Hyperacuity

1. Introduction

As Braddick (1993) points out in his excellent review, the human motion system faces two conflicting demands. To estimate object velocity with precision, the system should integrate over a fairly extensive spatiotemporal window. But an equally important function of motion processing is image segmentation, a major factor in breaking camouflage: discontinuities in the velocity flow field define the edges of surfaces. Optimal segmentation necessarily depends on good resolution. What is the balance between integration and resolution in human motion processing? To answer this question, we have measured the resolution of the motion system for a range of speeds, and determined the limitations this resolution imposes on the localization of motion discontinuities.

Early psychophysical studies (Loomis & Nakayama, 1973; Nakayama & Tyler, 1981; Nakayama, Silverman, MacLeod, & Mulligan, 1985; van Doorn & Koenderink, 1982) found motion resolution to be fairly coarse. Regan and Hong (1990) reported that Snellen acuity for motion-defined letters is 2–5′. Watson and Eckert (1994) measured the “motion-contrast sensitivity function” with a procedure similar to a conventional measurement of the contrast sensitivity function. They modulated spatial bandpass noise with sinusoidally varying motion, both in the direction of the edge (shear) and orthogonal to it (“compression”), and determined the amplitude of the modulation that could be discriminated from dynamic noise as a function of

* Corresponding author. Tel.: +39 348 3972198.
E-mail address: dave@in.cnr.it (D. Burr).

0042-6989/$ - see front matter
doi:10.1016/j.visres.2005.09.025

modulation frequency. For the highest spatial frequency bandwidth, the cutoff modulation frequency was 4–6 c/deg, suggesting that, for the slow speed (1 deg/s) studied, the smallest receptive field for a motion detector was about 10′, or a half-period resolution of ∼5′; their results for motion-defined square wave gratings gave somewhat higher cutoff frequencies. Resolution decreased with increasing speed agreeing with previous studies showing that the optimum spatial filter for motion varies with speed, increasing systematically with increasing speed (Burr & Ross, 1982; Kelly, 1979; van Doorn & Koenderink, 1982).

How does the poor resolution of the motion system affect edge localization by motion signals? Effectively, motion-defined edges are 'blurred' by the low-resolution motion detectors. Several studies have examined the effect of blur on localization for static targets. Typically, small amounts of blur have almost no effect on Vernier and spatial interval judgments. Once stimulus blur exceeds the internal noise ('intrinsic blur') of the visual system, thresholds rise monotonically (Levi & Klein, 1990; Watt & Morgan, 1984); thresholds rise as the square root of the standard deviation for Gaussian blur. As Watt and Morgan (1984) note, this pattern is consistent with a shift from fine to coarser spatial filters with increasing blur.

Importantly, the basic relationship between resolution and localization for luminance stimuli is unchanged by blur: at all values of blur, localization is about 3 times better than resolution (Levi & Klein, 1990). If this pattern holds for motion-defined edges, edge localization may be expected to be substantially better than resolution for motion-defined contours. Based on Watson and Eckert's estimate of resolution, motion-defined edges should be localized with a precision of 1–2′. Regan (1986) measured Vernier acuity for a random-dot target rendered visible from its background by differential motion; thresholds were ∼0.75′ for targets without residual luminance artifacts. Banton and Levi (1993) extended Regan's work to a wide range of dot densities and target sizes. Their best Vernier thresholds for motion-defined targets were 0.8–2′.

Previous studies have attempted to assess the size of the receptive fields of putative first-order motion detectors. In a series of studies, Anderson and Burr (1987, 1989, 1991; Anderson, Burr, & Morrone, 1991) used summation and masking techniques to estimate the length and height (spatial extent parallel and orthogonal to motion direction) of human motion detectors for a variety of speeds. Both techniques gave very similar results, suggesting that receptive fields of first-order motion detectors are not elongated in the direction of motion, being as high as they are wide. Size varies with spatial frequency, ranging from about 3′ (0.05 deg) at 10 c/deg to over 1 deg at 0.1 c/deg (but see also Fredericksen, Verstraten, & van de Grind, 1997).

This study has two major goals: first, to measure the resolution with which the human visual system can use motion information to segregate images, over a wide range of image speeds and spatial frequencies, and to relate these thresholds to previous estimates of receptive field size of primary motion mechanisms discussed above; and second, to examine the relationship between motion-defined resolution and motion-defined edge localization for identical stimulus configurations.

2. Methods

The stimuli used in this study were random noise patterns like those of Fig. 1, in which alternate horizontal regions were caused to drift in opposite directions at equal and constant speed (see also on-line videos). As the spatial statistics of the stimuli were identical everywhere, the regions could be discriminated solely on the basis of velocity differences. The width of the stripes, hence spatial frequency and number of stripes, varied from condition to condition (always "squarewave"). The basic stimuli comprised 512×512 pixels, 256 grey levels per pixel. Each pixel was 0.5×0.5 mm, subtending 1′ at 160 cm viewing distance.

Stimuli were generated by a dedicated VSG 2/5 framestore (Cambridge Research Systems) and displayed on the face of a Sony Trinitron monitor (24×24 cm, subtending 8.5° at 160 cm). Mean luminance was 30 cd/m^2 and monitor frame rate was 110 Hz. Motion stimuli were updated every two frames (55 Hz), to produce various drift speeds.

For most conditions, the stimuli were low-pass filtered in the horizontal dimension, in the direction of motion drift. The filter was Gaussian in frequency space. Figs. 1B–D show examples of filtered stimuli of different cutoff frequency, with cutoff frequency defined as the Gaussian space constant (where amplitude is reduced to 0.37 maximum).

Two types of resolution were measured, grating acuity and alignment acuity. For grating acuity, observers were required to discriminate in two interval-forced choice between a motion-contour-defined grating, and a stimulus of matched spatial frequency in which the motion was distributed uniformly over the entire field, creating an impression of two transparent sheets drifting over each other. In practice, the transparent stimulus was a very high frequency grating, 256 c/screen, with alternate raster lines drifting in opposite direction. Either the spatial frequency was varied from trial to trial to home in on resolution thresholds, or signal-to-noise ratio was varied to home in on coherence thresholds (both with the adaptive QUEST routine of Watson & Pelli, 1983). For the motion coherence measurements, signal (coherent motion) and noise (independent random stimuli) were presented on alternate frames (at 110 Hz). Signal-to-noise was then varied by varying the relative contrast of the two frames, keeping the total average contrast constant at maximum (50%). For the acuity measurements, contrast was kept constant at 50%. Coherence thresholds for direction discrimination were also measured, by requiring observers to discriminate the direction of stimulus motion, while coherence ratio was varied adaptively (one interval-forced choice).

For alignment thresholds, observers were required to judge whether the motion-defined contour was above or below screen centre (one interval-forced choice). To aid this

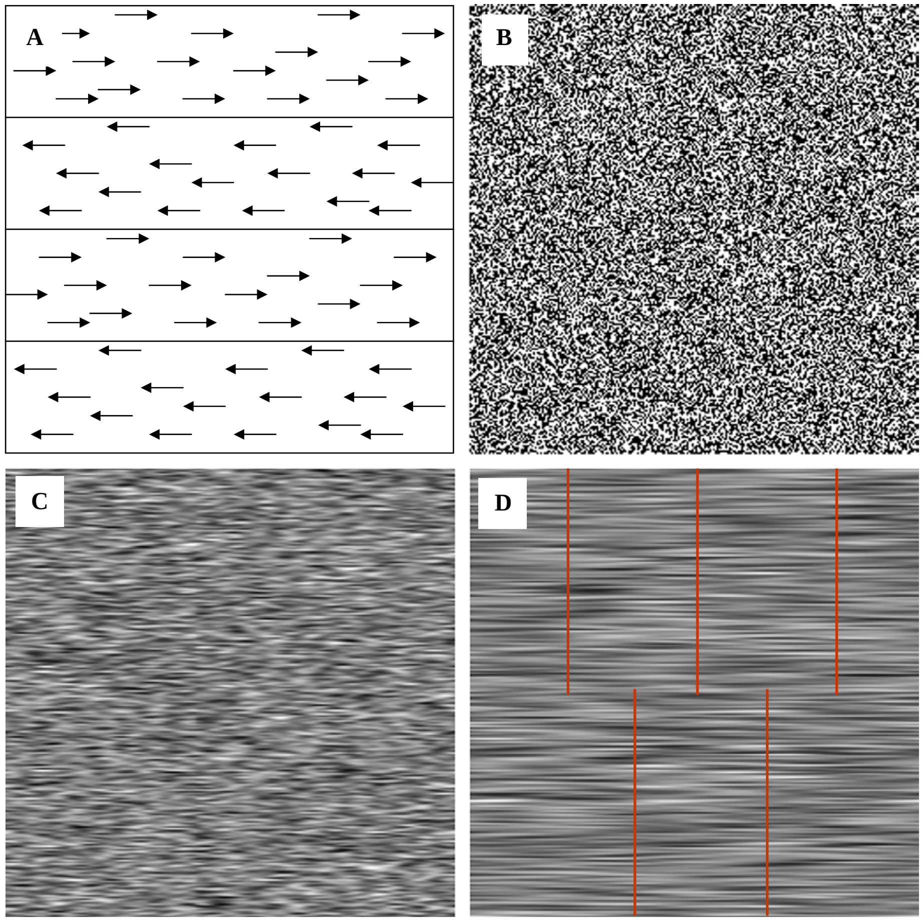

Fig. 1. (A) Schematic illustration of the stimuli used to measure grating resolution. Motion was of constant speed, but alternate stripes moved in opposite directions, defining clear regions (see also on-line movies). (B) Actual appearance of a single frame of unfiltered stimulus. There is mathematically no static spatial information to define the stripes seen when motion is introduced. (C) Example of stimuli filtered in the horizontal direction, with cutoff frequency of 1.6 c/deg (at the appropriate viewing distance). (D) Example of the stimulus used for the alignment thresholds. Observers had to judge whether the motion contour was above or below the end of the red lines. In this example, the stimulus is low-pass filtered at 0.4 c/deg. (For interpretation of the references to colour in this figure legend, the reader is referred to the web version of this paper.)

judgment, five thin red vertical lines terminated at screen centre (see Fig. 1D). All thresholds were calculated by fitting a cumulative Gaussian function to the psychometric functions, and calculating the point of 75% correct response. To allow direct comparison between different types of measurements, thresholds measured with two intervals of stimulus (grating acuity and coherence) were corrected by dividing by a factor of root-two (Geisler, 1984; Green & Swets, 1966).

Complete measurements were made primarily on two observers, author S.M. and P.B., naïve to the goals of the experiment. However, all major effects were verified informally by all authors. All observers had normal or corrected-to-normal acuity.

3. Results

3.1. Motion segregation

We first measured coherence thresholds for motion segregation as a function of the spatial frequency of the motion alternation. As detailed in methods, the task was to discriminate in 2AFC the structured motion-defined "grating" from one of purely transparent motion, matched in all respects except that the motion in the two directions was uniformly spread throughout the stimuli. For these measurements, the stimuli were unfiltered, with a drift speed of 4 deg/s.

Fig. 2 shows the results. For low spatial frequencies (less than 1–2 c/deg), the coherence thresholds were about 20%, virtually the same as the thresholds for direction discrimination. This result implies that when observers were able to discriminate the direction of motion reliably, they were also able to use that information to structure the stimulus and discriminate it from one of uniform transparency. For spatial frequencies above 2 c/deg, thresholds rose sharply. The last points of the curve are estimates of acuity for motion segregation. These measurements were made with stimuli of 100% coherence, varying in spatial frequency (hence the horizontal error-bars). For all three observers, the acuity was around 10 c/deg, corresponding to a threshold stripe width of 3′.

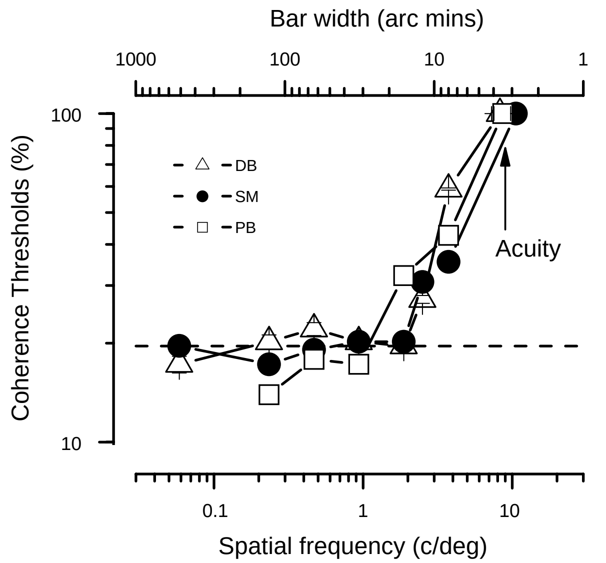

Fig. 2. Coherence thresholds for discriminating between a motion-defined grating from matched transparent motion, as a function of spatial frequency of the grating. The upper abscissa shows the width of the grating bars (half period) in arcmin. Image speed was 4 deg/s and the noise was unfiltered. The results are for three observers, one (PB) naïve to the goals of the experiment.

In all subsequent measurements we measured acuity thresholds with stimuli of 100% motion coherence. We firstly varied image speed, over a wide range (from 1 to 30 deg/s). The filled squares of Fig. 3 show how grating resolution thresholds vary with image speed. For both observers, thresholds remained fairly constant with speed up to 4 deg/s, then increased with speed, roughly linearly.

As there is a strong link between optimal speed and spatial frequency tuning (e.g., Burr & Ross, 1982), we investigated motion segregation with low-pass filtered stimuli. As described in methods, the spatial filtering was one-dimensional, only in the direction of motion (parallel to the segregating edges) so as not to blur the actual edge. The results are shown in Figs. 4A and B for four levels of low-pass filter, together with the unfiltered results (replotted from Fig. 3). For the highest cutoff frequency (6.4 c/deg), the results were very similar to the unfiltered stimuli, with thresholds increasing with speed for speeds higher than about 5 deg/s. For more severely blurred stimuli, the curves are "U-shaped," increasing both at high speeds and at low speeds. This pattern of results is consistent with the fact that lower spatial frequencies are best seen at higher image speeds, probably because of the temporal frequency tuning of the motion system (e.g., Burr & Ross, 1982). When data points are missing (such as for the low speeds of the low-pass filtered patterns), observers were unable to do the task at any bar width.

3.2. Alignment thresholds

The data so far study the resolution with which a dynamic pattern can be segregated on the basis of motion signals. Another important issue in spatial vision is the precision with which motion information can be used to localize the position of a contour in space. To measure this precision, we required subjects to discriminate whether a motion-defined border was higher or lower than the centre of the screen, clearly marked with five red stationary lines (Fig. 1D). Again, we first measured these thresholds for unfiltered stimuli as a function of image speed. Alignment thresholds (open circles of Fig. 3) for localizing the position of the edge follow closely those for segregation (filled symbols), both in absolute levels and in dependency on image speed.

We also repeated the measurements for one-dimensional low-pass filtered stimuli (similar to those used with the segregation studies). The results, shown in Figs. 4C and D, strongly resemble the pattern of results observed with motion segregation: thresholds for unfiltered or mildly filtered patterns increased with speed, while those for more heavily filtered pattern were U-shaped. Again this is consistent with lower spatial frequency mechanisms being selective to higher speeds.

Fig. 5 replots all the alignment thresholds from Figs. 4C and D against the grating thresholds of Figs. 4A and B (for matched conditions of image speed and spatial frequency) to bring out the relationship between the two thresholds. There is a clear and strong linear covariation between the two conditions, with r^2 of 0.8 for PB and 0.73 for SM. For both observers, grating thresholds were only slightly worse

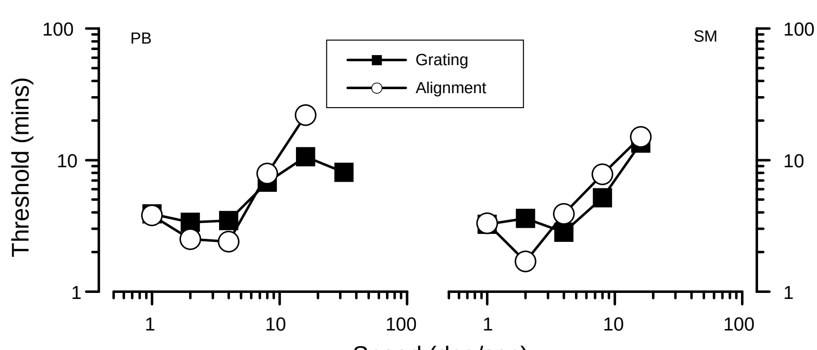

Fig. 3. Thresholds for grating segregation (filled squares) and for edge alignment (open circles) as a function of stimulus drift speed.

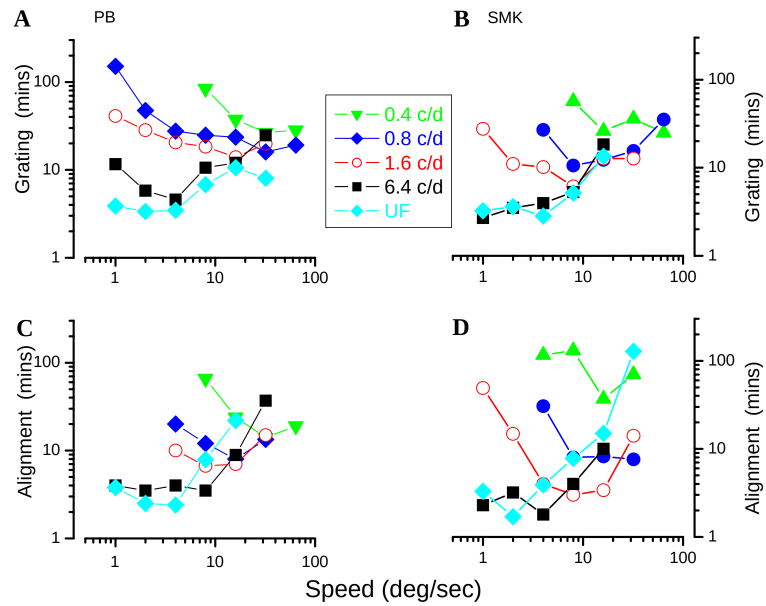

Fig. 4. (A,B) Thresholds for grating segregation for two observers and five different levels of low-pass filtering, as a function of drift speed. (C,D) Alignment thresholds for five different levels of low-pass filtering, as a function of drift speed.

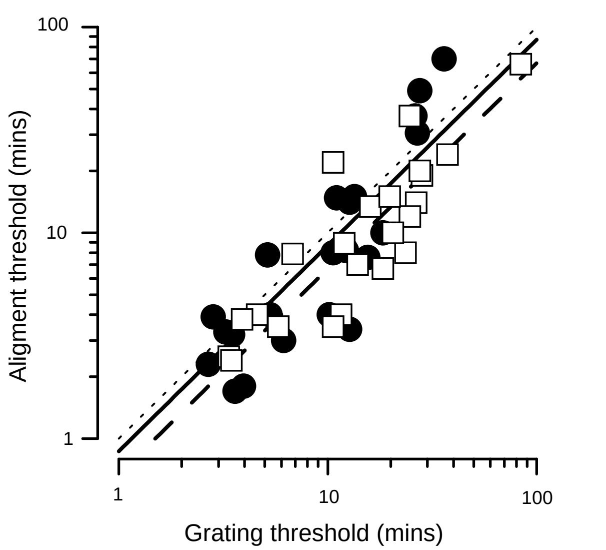

Fig. 5. Alignment thresholds (from Figs. 4A and B) plotted against segregation thresholds (from Figs. 4C and D) for all levels of low-pass filtering and drift speed. There was a strong covariance between the two measures, with r^2 of 0.8 for PB (open squares) and 0.73 for SM (filled circles). The solid line shows the best linear fit for the data (on logarithmic coordinates) for observer SM, dashed line for PB. The dotted diagonal line shows the equi-sensitivity prediction. On average, grating thresholds were only slightly worse than alignment thresholds, by a factor of 1.5 ± 0.04 log-units (SEM) for PB and 1.15 ± 0.05 log-units for SM (geometric averages).

than alignment thresholds, by a factor of 1.5 for PB and 1.15 for SM (geometric averages).

3.3. Comparing thresholds with receptive fields

As mentioned earlier, stimuli of different speeds are best detected by motion mechanisms with different preferred spatial frequency: high speeds are best detected at low spatial frequency (Anderson & Burr, 1985; Burr & Ross, 1982). It therefore seems reasonable to choose the best threshold for each spatial frequency, as representing the best performance that class of detector can do. Fig. 6 plots best grating and alignment thresholds as a function of blur cutoff for the two observers. Both thresholds fall monotonically with filter cutoff, from about 30′ at filter cutoff 0.4 c/deg to 2–3′ at 6 c/deg.

What may be the limiting factor for these motion-defined spatial thresholds? The most obvious limit for any threshold is the size of the relevant receptive fields. As the spatial border was parallel to the direction of motion, the most appropriate dimension would be the height of the receptive field. The black symbols of Fig. 6 plot estimates of receptive field height, taken from previous data of Anderson and colleagues (Anderson & Burr, 1991; Anderson, Burr, & Morrone, 1991), using two different techniques, summation and masking: the summation measurements looked for the critical size summation size for sinusoidal gratings varying in height, the masking estimates from inverse-transform of measurements of two-dimensional masking of drifting sinusoidal gratings. Although these data were taken under quite different conditions (brighter luminance, use of sinusoidal gratings rather than filtered noise etc), the estimates of receptive field height fall remarkably close to the estimates of segregation and alignment thresholds of this study.

4. Discussion

This paper establishes several facts. First, the results confirm many previous studies in showing that motion information can provide very strong and robust cues for spatial

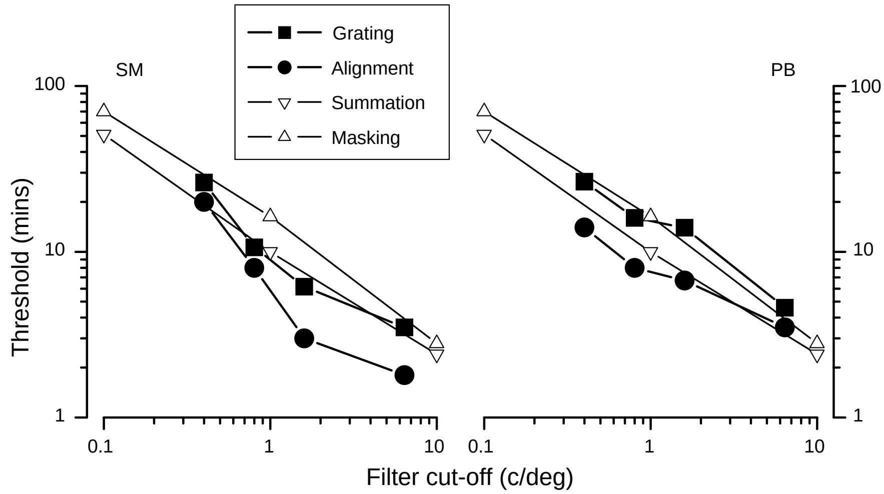

Fig. 6. Best grating (filled squares) and alignment (filled circles) acuity as a function of low-pass filter cutoff frequency (from Fig. 4). The inverted and upright triangles show the average estimates for the height of first-order motion receptive fields, derived respectively from summation and masking (taken from Anderson and Burr, 1991; Anderson et al., 1991). There is reasonable agreement between the data of this study, and the previous estimates of receptive field size.

segregation. For large stripe widths (greater than 2 deg), the coherence thresholds for motion segregation were the same as those for detecting motion direction under these conditions, about 20% (in agreement with Tsujimura & Zaidi, 2002). The best acuity thresholds for motion-defined gratings were 2.8 and 3.4′, agreeing well with Watson and Eckert's (1994) estimates for square wave gratings. The thresholds are better than many early estimates (Loomis & Nakayama, 1973; Nakayama & Tyler, 1981; Nakayama et al., 1985; van Doorn & Koenderink, 1982), possibly because the speeds and other parameters were not optimal in those studies.

As may be expected, resolution thresholds varied both with drift speed and with spatial frequency filtering. For unfiltered stimuli, resolution was fairly constant up to 4 deg/s, but increased with higher drift speeds, roughly linearly. Low-pass filtering also affected thresholds (as Watson & Eckert, 1994 showed), even though the filtering was orthogonal to the direction of the edge so as not to blur the actual edge. For filtered stimuli, best resolution occurred at higher drift speeds, consistent with evidence that higher speeds are detected by mechanisms tuned to lower spatial frequency (Anderson & Burr, 1985; Burr & Ross, 1982). When the best thresholds are taken for each filtered image, thresholds increased with cutoff frequency following a roughly square-root relationship.

An obvious question to ask is what is limiting these thresholds. Watson and Eckert (1994) suggested that integration may be limited by the properties of first-stage mechanisms, and our results support this idea. Fig. 6 shows compares the segregation thresholds of this study with previous estimates of the size of receptive fields of putative first-order motion detectors, obtained from contrast sensitivity measurements with sinusoid gratings. These data were obtained with two separate techniques: increasing the height of a drifting grating until sensitivity saturated; and by inverse transform of masking data. There are clearly difficulties in making stringent quantitative comparisons between the old measurements of receptive field size and the present data, for a number of reasons. The previous experiments used different observers, narrow bandwidth sinusoidal gratings (compared with broadband low-pass stimuli of the current study), and far higher luminances (400 cd/m^2 compared with 30 cd/m^2). Nevertheless, there is a remarkable consistency between the estimates of receptive field height and the resolution thresholds of the current study. Over a very wide range of spatial frequency cutoff frequencies, the grating resolution thresholds for both observers fall in the range of the two estimates of receptive field size. Both the dependency on spatial frequency, and the absolute size estimates are in remarkable agreement, suggesting that resolution of motion segregation is limited by the spatial extent of first-order mechanisms, without needing to invoke any higher-order integration stages.

The suggestion that motion segregation thresholds are limited by first-order motion mechanisms agrees with several physiological studies. Lamme and colleagues (Lamme, 1995; Lamme, van Dijk, & Spekreijse, 1993) recorded strong visual evoked potentials elicited in area V1 in both monkeys and humans in response to motion-defined contours. With functional magnetic resonance imaging, Reppas, Niyogi, Dale, Sereno, and Tootell (1997) showed that V1 responds to motion-defined contours retinotopically. The results also agree with Watson and Eckert (1994) who, largely on the basis of modelling first-order responses, rejected the need for higher-order integration prior to motion segregation. They also found that under the conditions of their experiment, segregation thresholds for motion shear (parallel to the motion contour, as used in this study) were similar to those for motion "compression" (orthogonal to the motion contour). Again this is consistent with the summation and masking results (Anderson & Burr, 1991; Anderson et al., 1991) that show that receptive fields for motion detectors are circular, as high as they are wide (similar spatial extent parallel and orthogonal to motion direction).

The fact that the thresholds are well predicted by first-order motion mechanisms, and the clear involvement of V1 with motion contours does not preclude totally the involvement of higher-order motion centres. Sinha (2001) has recently shown that the strength of motion-defined contours depends on disambiguation of plaids, a process that is thought to occur at higher levels of motion processing, probably in MT (Movshon, Adelson, Gizzi, & Newsome, 1985). As Sinha points out, it is not unreasonable to assume that motion information at various levels can contribute to the formation of contours, given their importance for mammalian vision.

Given the conflicting tasks of a motion system—integration and segmentation (Braddick, 1993)—it is reasonable that segregation should be limited by early first-order mechanisms. In order for the image to be segregated, motion needs to be detected and coded, a task that requires motion selective mechanisms. Resolution can never be better than the spatial resolution of these detectors. To increase sensitivity and to create detectors selective to more complex forms of motion (for example radial and circular), output from low-level detectors must be integrated further (Burr, Morrone, & Vaina, 1998; Morrone, Burr, & Vaina, 1995). However, the best segregation performance will use information prior to this further integration stage, and could also follow different neuronal pathways.

Thresholds for motion alignment followed closely those for grating segregation, for all image speeds and filter cutoffs (see Fig 5). Performance was slightly better for alignment thresholds than for grating resolution, but only by a factor of 1.5 for PB and 1.15 for SM. But importantly, this ratio remained constant for all image blurs, as Levi and Klein (1990) found for luminance-defined thresholds. What was different, however, is that they found localization thresholds to be three times better than acuity thresholds, whereas the results here suggest that localization thresholds for motion-defined contours are only 1–1.5 times better than acuity thresholds. Note that every effort was made to facilitate edge localization, including the addition of red markers to help the bisection. We should also stress that the thresholds values for grating acuity were corrected by a factor of root-two for the fact that a two interval-forced choice technique was used for that task, whether the alignment acuity used only one temporal interval. It is not clear why motion-defined edge localization should be worse than luminance-defined localization (relative to acuity thresholds), but is does suggest that the luminance system is more specialized for edge localization (see for example Klein & Levi, 1985; Wilson, 1986).

In the natural world, motion can be a fundamental cue for segregating images, and for locating these segregated images in space, partly under conditions of camouflage, where other cues such as luminance bounders are rendered ineffective. The current study supports much previous work in showing that the human visual system is well equipped to take advantage of motion signals to perform this segregation and localization reliably and robustly, and with moderately good acuity. The acuity is clearly poorer than for the luminance system can achieve, by a factor of 5–10, but it is nevertheless operates in the region of minutes rather than degrees of arc, probably making a valuable contribution to image segmentation and localization under natural viewing conditions.

Appendix A. Supplementary data

Please note that these movies are intended only to illustrate the stimuli and are not precise reproductions of the actual experiments. The appearance will depend on several factors, including the resolution and type of monitor used. Supplementary data associated with this article can be found, in the online version, at doi:10.1016/j.visres.2005.09.025.

References

Anderson, S. J., & Burr, D. C. (1985). Spatial and temporal selectivity of the human motion detection system. *Vision Research, 25*, 1147–1154.

Anderson, S. J., & Burr, D. C. (1987). Receptive field sizes of human motion detectors. *Vision Research, 27*, 621–635.

Anderson, S. J., & Burr, D. C. (1989). Receptive field properties of human motion detector units inferred from spatial frequency masking. *Vision Research, 29*, 1343–1358.

Anderson, S. J., & Burr, D. C. (1991). Receptive field length and width of human motion detector units: Spatial summation. *Journal of the Optical Society of America. A, 8*, 1330–1339.

Anderson, S. J., Burr, D. C., & Morrone, M. C. (1991). The two-dimensional spatial and spatial frequency properties of motion sensitive mechanisms in human vision. *Journal of the Optical Society of America. A, 8*, 1340–1351.

Banton, T., & Levi, D. M. (1993). Spatial localization of motion-defined and luminance-defined contours. *Vision Research, 33*(16), 2225–2237.

Braddick, O. (1993). Segmentation versus integration in visual motion processing. *Trends in Neurosciences, 16*, 263–268.

Burr, D. C., Morrone, M. C., & Vaina, L. (1998). Large receptive fields for optic flow direction in humans. *Vision Research, 38*, 1731–1743.

Burr, D. C., & Ross, J. (1982). Contrast sensitivity at high velocities. *Vision Research, 23*, 3567–3569.

Fredericksen, R. E., Verstraten, F. A., & van de Grind, W. A. (1997). Pitfalls in estimating motion detector receptive field geometry. *Vision Research, 37*(1), 99–119.

Geisler, W. S. (1984). Physical limits of acuity and hyperacuity. *Journal of the Optical Society of America. A, 1*(7), 775–782.

Green, D. M., & Swets, J. A. (1966). *Signal detection theory and psychophysics*. New York: John Wiley & sons.

Kelly, D. H. (1979). Motion and vision. II. Stabilized spatio-temporal threshold surface. *Journal of the Optical Society of America, 69*(10), 1340–1349.

Klein, S. A., & Levi, D. M. (1985). Hyperacuity thresholds of 1 s: Theoretical predictions and empirical validation. *Journal of the Optical Society of America. A, 2*, 1170–1190.

Lamme, V. A. (1995). The neurophysiology of figure-ground segregation in primary visual cortex. *Journal of Neuroscience, 15*(2), 1605–1615.

Lamme, V. A., van Dijk, B. W., & Spekreijse, H. (1993). Contour from motion processing occurs in primary visual cortex. *Nature, 363*(6429), 541–543.

Levi, D. M., & Klein, S. A. (1990). Equivalent intrinsic blur in spatial vision. *Vision Research, 30*(12), 1971–1993.

Loomis, J. M., & Nakayama, K. (1973). A velocity analogue of brightness contrast. *Perception, 2*(4), 425–427.

Morrone, M. C., Burr, D. C., & Vaina, L. (1995). Two stages of visual processing for radial and circular motion. *Nature, 376*, 507–509.

Movshon, J. A., Adelson, E. H., Gizzi, M. S., & Newsome, W. T. (1985). The analysis of moving visual patterns. In: R. G. C. Chagas, C. Gross (Eds.) *Pattern Recognition Mechanisms*, Vol. 54 (pp. 117–151). Pontificiae Academiae Scientiarum Scripta Varia.

Nakayama, K., Silverman, G. H., MacLeod, D. I., & Mulligan, J. (1985). Sensitivity to shearing and compressive motion in random dots. *Perception, 14*(2), 225–238.

Nakayama, K., & Tyler, C. W. (1981). Psychophysical isolation of movement sensitivity by removal of familiar position cues. *Vision Research, 21*(4), 427–433.

Regan, D. (1986). Form from motion parallax and form from luminance contrast: Vernier discrimination. *Spatial Vision, 1*(4), 305–318.

Regan, D., & Hong, X. H. (1990). Visual acuity for optotypes made visible by relative motion. *Optometry and Vision Science, 67*(1), 49–55.

Reppas, J. B., Niyogi, S., Dale, A. M., Sereno, M. I., & Tootell, R. B. (1997). Representation of motion boundaries in retinotopic human visual cortical areas. *Nature, 388*(6638), 175–179.

Sinha, P. (2001). Role of motion integration in contour perception. *Vision Research, 41*(6), 705–710.

Tsujimura, S., & Zaidi, Q. (2002). Similarities between visual processing of shear and uniform motion. *Vision Research, 42*(28), 3005–3017.

van Doorn, A. J., & Koenderink, J. J. (1982). Visibility of movement gradients. *Biological Cybernetics, 44*(3), 167–175.

Watson, A. B., & Eckert, M. P. (1994). Motion-contrast sensitivity: Visibility of motion gradients of various spatial frequencies. *Journal of the Optical Society of America, 11*, 496–505.

Watson, A. B., & Pelli, D. G. (1983). QUEST: a Bayesian adaptive psychometric method. *Perception & Psychophysics, 33*(2), 113–120.

Watt, R. J., & Morgan, M. J. (1984). Spatial filters and the localization of luminance changes in human vision. *Vision Research, 24*, 1139–1387.

Wilson, H. R. (1986). Responses of spatial mechanisms can explain hyperacuity. *Vision Research, 26*(3), 453–469.